Conformational Behavior of Sucrose and Its Deoxy Analogue in Water as Determined by NMR and Molecular Modeling

Catherine Hervé du Penhoat,[†] Anne Imberty,*[,‡] Nathalie Roques,[§] Véronique Michon,[†] Julio Mentech,[§] Gérard Descotes,[⊥] and Serge Pérez[‡]

Contribution from the Service RMN du Département de Chimie, U.A. 01110, E.N.S., 46 rue d'Ulm, 75230 Paris, France, Laboratoire de Physicochimie des Macromolécules, INRA, BP527, 44026 Nantes, France, Laboratoire Beghin-Say. E.S.C.I.L., 43 Bd du 11 Novembre 1918, 69622 Villeurbanne, France, and Laboratoire de Chimie Organique II. E.S.C.I.L., 43 Bd du 11 Novembre 1918, 69622 Villeurbanne, France. *Received March 13, 1990*

Abstract: The conformational behavior of aqueous sucrose and its 2-deoxy analogue were studied by NMR and computerized molecular modeling. ^1H steady-state NOE and NOESY data are reported along with long-range ^{13}C-^1H coupling constants. In modeling calculations, a full force field energy minimization was used to obtain the initial residue geometry, followed by a rigid residue approximation in which the glycosidic dihedral angles and the methoxyl group orientations are varied. Theoretical steady-state NOEs are calculated by a full spin relaxation matrix method, and $^3J_{C-H}$ data are correlated with the glycosidic torsional angle. The data do not support a single conformation model, and only conformational averaging can give a good agreement between theoretical and experimental data. The inclusion of hydrogen bonding in the force field does not affect the statistical weights of calculated NOEs, and the similar values of observed NOEs for sucrose and the 2-deoxy analogue argue against the importance of hydrogen bonding in sucrose conformation.

Introduction

The molecular conformation in crystalline sucrose is known unambiguously through X-ray[1] and neutron diffraction[2] studies. However, the conformational behavior of sucrose in aqueous solution is still controversial, despite numerous experimental[3-11] and modeling[12,13] studies. In most of those efforts,[6-9,11-13] sucrose was assumed to be nearly spherical, similar to its shape in crystalline sucrose, and quite rigid. However, when the crystal structures of sucrose,[1,2] sucrose–salt complexes,[14,15] and oligosaccharides that contain sucrosyl residues[16-22] are examined, the (1 ↔ 2) glycosidic linkages between α-glucopyranose and β-fructofuranose exhibit wide ranges (see Table I). Recent molecular mechanics and dynamics studies[23,24] identified three low-energy conformations for sucrose, providing further support for the concept of flexible linkages in this disaccharide.

Besides the flexibility of sucrose, another controversy is the persistence in solution of the O-2g–O-1f and O-5g–O-6f hydrogen bonds found in the crystal. Mathlouti et al.[3-5] interpreted X-ray and Raman data to show that the number of intramolecular hydrogen bonds depends on the concentration of sucrose, with no hydrogen bonding at low concentrations. Bock and Lemieux[11,12] argued, supported by modeling and detailed ^{13}C T_1 and NOE measurements, that dilute aqueous sucrose has one intramolecular hydrogen bond. Finally, based on their NMR study of sucrose in DMSO, Christofides and Davies[6,7] suggested that two intramolecular hydrogen bonds, namely O-2g–O-1f and O-2g–O-3f, compete with each other.

Because of these observations and a report that the crystalline conformation cannot account for all of the NMR data,[10] we decided that further study was needed. Interpreting the solution behavior of sucrose from NMR data without an assumption of rigid conformation is an ambitious task, since NMR parameters reflect only a "virtual" conformation.[25] Recently, Cumming and Carver[26] combined NMR data with results from computerized molecular modeling that accommodates conformational flexibility. Further analyses of various di- and trisaccharides have mostly used NOE values[27-29] although constants from coupling through the glycosidic linkage were also useful.[30-32] This modeling procedure is used in the present work. The extent of intramolecular hydrogen bonding is probed in a parallel study of 2-deoxysucrose, a compound that cannot form the O-1f–O-2g hydrogen bond. Also, the potential energy functions were used with and without a term for hydrogen bonding.

[†] Service RMN du Département de Chimie.
[‡] Laboratoire de Physicochimie des Macromolécules.
[§] Laboratoire Beghin-Say. E.S.C.I.L.
[⊥] Laboratoire de Chimie Organique II. E.S.C.I.L.

(1) Hanson, J. C.; Sieker, L. C.; Jensen, L. H. *Acta Crystallogr.* **1973**, *B29*, 797-808.
(2) Brown, G. M.; Levy, H. A.; *Acta Crystallogr.* **1973**, *B29*, 790-797.
(3) Mathlouthi, M. *Carbohydr. Res.* **1981**, *91*, 113-123.
(4) Mathlouthi, M.; Luu, D. V. *Carbohydr. Res.* **1980**, *81*, 203-212.
(5) Mathlouthi, M.; Luu, C.; Meffroy-Biget, A. M.; Luu, D. V. *Carbohydr. Res.* **1980**, *81*, 213-233.
(6) Christofides, J. C.; Davies, D. B. *J. Chem. Soc., Chem. Commun.* **1985**, 1533-1534.
(7) Davies, D. B.; Christofides, J. C. *Carbohydr. Res.* **1987**, *163*, 269-274.
(8) McCain, D. C.; Markley, J. L. *Carbohydr. Res.* **1986**, *152*, 73-80.
(9) McCain, D. C.; Markley, J. L. *J. Am. Chem. Soc.* **1986**, *108*, 4259-4264.
(10) Mulloy, B.; Frenkiel, T. A.; Davies, D. B. *Carbohydr. Res.* **1988**, *184*, 39-46.
(11) Lemieux, R. U.; Bock, K. *Jpn. J., Antibiot.* **1979**, XXXII Suppl., S163-S172.
(12) Bock, K.; Lemieux, R. U. *Carbohydr. Res.* **1982**, *100*, 63-74.
(13) Giacomini, M.; Pullman, B.; Maigret, B. *Theor. Chim. Acta* **1970**, *19*, 347-364.
(14) Accorsi, C. A.; Bellucci, F.; Bertolasi, V.; Ferretti, V.; Gilli, G. *Carbohydr. Res.* **1989**, *191*, 105-116.
(15) Accorsi, C. A.; Bertolasi, V.; Ferretti, V.; Gilli, G. *Carbohydr. Res.* **1989**, *191*, 91-104.
(16) Berman, H. M. *Acta Crystallogr.* **1970**, *B26*, 290-299.
(17) Rohrer, D. C. *Acta Crystallogr.* **1972**, *B28*, 425-433.
(18) Jeffrey, G. A.; Park, Y. J. *Acta Crystallogr.* **1972**, *B28*, 257-267.
(19) Avenel, D.; Neuman, A.; Gillier-Pandraud, H. *Acta Crystallogr.* **1976**, *B32*, 2598-2605.
(20) Becquart, J.; Neuman, A.; Gillier-Pandraud, H. *Carbohydr. Res.* **1982**, *111*, 9-21.
(21) Ferretti, V.; Bertolasi, V.; Gilli, G. *Acta Crystallogr.* **1984**, *C40*, 531-535.
(22) Gilardi, R.; Flippen-Anderson, J. L. *Acta Crystallogr.* **1987**, *C43*, 806-808.
(23) Tran, V.; Brady, J. W. *Biopolymers* **1990**, *29*, 961-976.
(24) Tran, V.; Brady, J. W. *Biopolymers* **1990**, *29*, 977-997.
(25) Jardetsky, O. *Biochim. Biophys. Acta* **1980**, *621*, 227-232.
(26) Cumming, D. A.; Carver, J. P. *Biochemistry* **1987**, *26*, 6664-6676.
(27) Breg, J.; Kroon-Batenburg, L. M. J.; Strecker, G.; Montreuil, J.; Vliegenthart, J. F. G. *Eur. J. Biochem.* **1989**, *178*, 727-739.
(28) Lipkind, G. M.; Shashkov, A. S.; Nechaev, O. A.; Torgov, V. I.; Shibaev, V. M.; Kochetkov, N. K. *Carbohydr. Res.* **1989**, *195*, 11-25.
(29) Carver, J. P.; Mandel, D.; Michnick, S. W.; Imberty, A.; Brady, J. W. In *Computer Modeling of Carbohydrate Molecules*; French, A. D., Brady, J. W., Eds.; ACS Symposium Series; American Chemical Society: Washington, DC, 1990; pp 266-280.

0002-7863/91/1513-3720$02.50/0

Table I. Review of the Crystal Structures of Sucrose, Sucrose–Salts, and Other Molecules Containing the Sucrose Moiety, along with the Geometrical Features of Interest and the Observed Hydrogen Bonds

ref	year	compound	τ, (deg)	Φ (deg)	Ψ (deg)	ω_g	ω_f	χ^f	glucose ring	fructose ring	hydrogen bonds
1	1963	sucrose	114.3	107.8	−44.8	GG	GG	TG	$^4C_1$	$^4T_3$	O-2g···O-1f
2	1973										O-5g···O-6f
16	1970	raffinose	122.2	81.7	11.4	GG	GT	GG	$^4C_1$	$^4T_3$	no
17	1972	planteose	118.9	108.6	−26.7	GT	GT	GG	$^4C_1$	$^4T_3$	no
18	1972	1-kestose	119.4	84.6	−65.9	GG	GT	TG	$^4C_1$	E_4	no
19	1978	melezitose I	119.3	99.8	−30.7	GG	GG	GG	$^4C_1$	$^4T_3$	O-5g···O-6f
20	1982	melezitose II	115.3	109.6	−43.4	GG	GT	GG	$^4C_1$	E_3	no
21	1984	6-kestose	121.3	89.6	−54.5	GT	GT	GG	$^4C_1$	$^4T_3$	no
22	1987	stachyose	117.7	108.8	−47.9	GG	GG	TG	$^4C_1$	$^4T_3$	O-2g···O-1f
											O-5g···O-6f
14	1989	NaBr, sucrose	116.7	99.8	−46.1	GG	GG	GG	$^4C_1$	E^4	O-1g···O-3f
15	1989	3NaI, 2 sucrose	118.8	79.9	−66.6	GT	GT	TG	$^4C_1$	E^4	no
			117.9	79.6	−61.6	GT	GT	TG	$^4C_1$	$^4T_5$	no

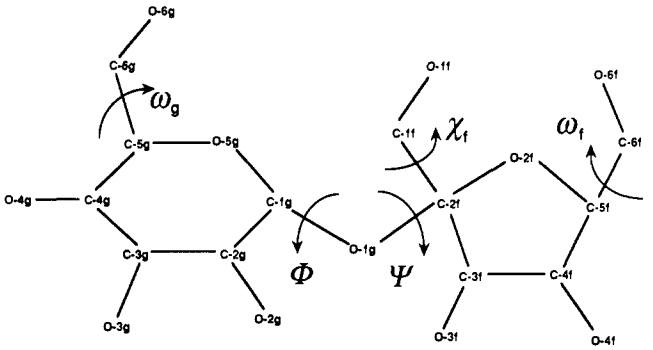

Figure 1. Sucrose with labels for the atoms and torsional angles of interest. Hydroxyl hydrogen atoms are not shown.

Materials and Methods

Material. 2-Deoxysucrose was prepared from 1′,2:4,6-di-*O*-isopropylidene-3,3′,4′,6′-tetra-*O*-acetylsucrose according to a literature procedure.[33] Solutions of this compound and reagent grade sucrose were prepared in D_2O (99.96%, SST).

Nomenclature. Sucrose and its atomic labels of interest are in Figure 1. The conformations about the glycosidic linkage bonds are described by the following torsion angles

$$\Phi = \theta(\text{O-5g–C-1g–O-1g–C-2f})$$

$$\Psi = \theta(\text{C-1g–O-1g–C-2f–O-5f})$$

The orientation of the three hydroxymethyl groups are described by the torsion angles ωg, ωf, χf. The orientation of the O-6g and O-6f primary

$$\omega g = \theta(\text{O-5g–C-5g–C-6g–O-6g})$$

$$\omega f = \theta(\text{O-5f–C-5f–C-6f–O-6f})$$

$$\chi f = \theta(\text{O-5f–C-2f–C-1f–O-1f})$$

alcohol groups are referred to as either gauche–gauche (GG), gauche–trans (GT), or trans–gauche (TG) with respective values of −60°, 60°, and 180° for the ω torsion angle. In this terminology the torsion angle θ(O-5–C-5–C-6–O-6) is stated first and θ(C-4–C-5–C-6–O-6) second.[34] The GT, GG, and TG terms are also used with O-1f primary alcohol group, based on the torsion angles O-5f–C-2f–C-1f–O-1f and C-3f–C-2f–C-1f–O-1f, respectively. The sign of torsion angles is defined in agreement with the recommendations of the IUPAC-IUB Commission of Biochemical Nomenclature.[35]

NMR Spectroscopy. The NMR spectra were recorded with a Bruker AM-400 instrument operating in the Fourier-transform mode at 296 K. Dissolved oxygen was removed by repeated evacuation, and the tubes were then sealed. The $^3J_{H-H}$ coupling constants were obtained from spectra acquired with 0.1-Hz digital resolution. Assignment of the ^1H signals of 2-deoxysucrose was obtained from the COSY spectrum.

Steady-state NOE difference spectra[36] were obtained from 0.06 M sucrose and 0.03 M 2-deoxysucrose solutions in D_2O. Two sets of measurements were made with irradiation times and pulse intervals greater than 5 times the longest T_1 for the sugar signals. There were 512 difference FIDs which were accumulated and Fourier transformed with an exponential line broadening factor of 1 Hz in order to reduce noise. Values from two spectra were averaged, and experimental error should be comparable to that reported in the literature.[27]

Phase-sensitive NOESY[37] spectra were acquired with mixing times of 0.1, 0.2, 0.25, 0.3, 0.35, 0.4, and 1.25 s. 512 × 1 K data matrices were obtained and zero-filled to 1K × 1K. Prior to Fourier transformation the first data file was halved to reduce t_1 ridges, and $\pi/2$-shifted sine-squared weighting functions were applied.[38] NOESY crosspeaks intensities were evaluated from the summed ω_1 subspectra contributing to a specific signal.

T_1 measurements used the inversion-recovery pulse sequence (180°–τ–90°–AT–PD) where AT represents the signal acquisition time and PD is the pulse delay (AD + PD = $5T_1$).[12] Variable delay (τ) values were used, and T_1 was determined by using the Bruker software subroutine.

For the selective heteronuclear 2D *J*-resolved[39] spectra, 64 × 2 K data matrices were obtained with the total evolution period varied up to 1.6 s giving a 20-Hz spectral width in ω_1. No apodization function was used in ω_2, and zero-filling gave 128 × 2 K data matrices prior to Fourier transformation. Slices corresponding to ^{13}C lines were multiplied by both a negative 3-Hz line-narrowing factor and a 0.25-Hz Gaussian function before Fourier transformation.

Calculations of NOE and Coupling Constants from a Computer Model. The full relaxation matrix method[40] for computing the NOE values was published earlier[26] and will not be described here. Coupling constants ($^3J_{H-C}$) across the glycosidic bond were calculated by using a newly proposed Karplus-type equation for the C–O–C–H segment.[41]

$$^3J_{C-H} = 5.7 \cos^2 \theta_H - 0.6 \cos \theta_H + 0.5$$

Averaging is required to correctly predict properties for our population of low-energy computer models distributed over p conformational states. The relative population of the ith conformational state, P_i, with energy, E_i, is dictated by the Boltzmann distribution

$$P_i = \exp(-E_i/kT)/\sum \exp(-E_i/kT)$$

By using the fractional population for each conformational microstate, the average coupling constant can be computed from

$$\langle ^3J_{C-H} \rangle = \sum P_i {}^3J_{iC-H}$$

For NOEs, the method for averaging depends on the rate of conformational exchange. Exchange for disaccharides is fast compared to the isotropic rotational correlation time (τ_c), so averaging was done over all values of the inverse sixth power of the interproton distances. This is equivalent to averaging the elements of the relaxation matrix. Only the

(30) Perez, S.; Taravel, F. R.; Vergelati, C. *Nouv. J. Chim.* **1985**, *9*, 561–564.
(31) Cumming, D. A.; Carver, J. P. *Biochemistry* **1987**, *26*, 6676–6683.
(32) Tvaroska, I.; Imberty, A.; Perez, S. *Biopolymers* **1990**, *30*, 369–379.
(33) Descotes, G.; Mentech, J.; Rocques, N. *Carbohydr. Res.* **1989**, *188*, 63–70.
(34) Marchessault, R. H.; Perez, S. *Biopolymers* **1979**, *18*, 2369–2374.
(35) IUPAC-IUB, Commission on Biochemical Nomenclature, *Arch. Biochem. Biophys.* **1971**, *145*, 405–421; *J. Mol. Biol.* **1970**, *52*, 1–17.
(36) Richarz, R.; Wüthrich, K. *J. Magn. Reson.* **1975**, *30*, 147–150.
(37) Macura, S.; Huang, Y.; Suter, D.; Ernst, R. R. *J. Magn. Reson.* **1981**, *43*, 259–281.
(38) Neuhaus, D.; Williamson, M. In *The Nuclear Overhauser Effect in Structural and Conformational Analysis*; VCH Publishers: 1989; p 292.
(39) Morat, C.; Taravel, F. R.; Vignon, M. R. *Magn. Reson. Chem.* **1988**, *26*, 264–270.
(40) Noggle, J. H.; Schirmer, R. E. In *The Nuclear Overhauser Effect*; Academic Press: New York, 1971.
(41) Tvaroska, I.; Hricovini, M.; Petrakova, E. *Carbohydr. Res.* **1989**, *189*, 359–362.

Table II. 400-MHz ^1H Chemical Shifts (ppm) and Observed $^3J_{H-H}$ Coupling Constants (Hz) for 0.06 M Sucrose and 0.03 M 2-Deoxysucrose in D_2O (d_{HDO} = 4.8 ppm)[e]

proton	δ	T_1	exptl J	calc J	Δ_J
		Sucrose			
H-1g ($J_{H\cdot1g-H\cdot2g}$)	5.39	0.92	3.8	3.6[a]	0.2
H-2g ($J_{H\cdot2g-H\cdot3g}$)	3.53	1.18	10.0	9.9[a]	0.1
H-3g ($J_{H\cdot3g-H\cdot4g}$)	3.73	1.57	9.1	9.4[a]	0.3
H-4g ($J_{H\cdot4g-H\cdot5g}$)	3.44	1.36	9.8	9.8[a]	0.0
H-5g	3.86				
H-6ga, H-6gb	3.76–3.81				
H-1f (a + b)	3.61	0.38			
H-3f ($J_{H\cdot3f-H\cdot4f}$)	4.19	1.66	8.8	7.8[b]	1.0
H-4f ($J_{H\cdot4f-H\cdot5f}$)	4.02	1.24	8.3	8.9[c]	0.6
H-5f	3.83				
H-6fa, H-6fb	3.76–3.81				
		2-Deoxysucrose			
H-1g ($J_{H\cdot1g-H\cdot2ga}$)	5.52		3.5	3.1[a]	0.4
($J_{H\cdot1g-H\cdot2ge}$)			1.2	1.3[a]	0.1
H-2ga ($J_{H\cdot2ga-H\cdot3g}$)	1.71		12.0	12.0[a]	0.0
H-2ge ($J_{H\cdot2ge-H\cdot3g}$)	2.03		5.0	4.9[a]	0.1
H-3g ($J_{H\cdot3g-H\cdot4g}$)	3.96		9.2	9.3[a]	0.1
H-4g ($J_{H\cdot4g-H\cdot5g}$)	3.38		9.2	9.7[a]	0.5
H-5g	3.80				
H-6ga, H-6gb	3.76–3.80				
H-1f (a + b)	3.65				
H-3f ($J_{H\cdot3f-H\cdot4f}$)	4.15		8.8	8.0[b]	0.8
H-4f ($J_{H\cdot4f-H\cdot5f}$)	4.04		8.0	8.9[c]	0.9
H-5f	3.83				
H-6fa, H-6fb	3.76–3.80				

[a] Calculated from Altona and Haasnoot equation.[40] [b] Calculated from $^3J_{H\cdot3f-H\cdot4f}$ = 4.35 cos 2Φ − 0.91 cos Φ + 2.34 sin 2Φ + 4.83. [c] Calculated from $^3J_{4H\cdot4f-H\cdot5f}$ = 3.97 cos 2Φ − 0.91 cos Φ − 0.10 sin 2Φ + 4.67. [d] Equations for *b* and *c* were established from ref 52. [e] The calculated $^3J_{H-H}$ coupling constants along with the difference between experimental and theoretical values, Δ_J, are also reported. ^1H T_1 (s) are reported for the sucrose molecule.

conformations having an energy value less than 20 Kcal/mol were taken into account in these averaging procedures.

$$\langle r(k,l)^{-6} \rangle = \sum P_i r_i(k,l)^{-6}$$

Conformational Analysis. Two different molecular mechanics programs were used. First, MMP2(85)[42] was used to optimize the atomic coordinates taken from the crystal structure. This provided a structure devoid of intermolecular influence. Following optimization, the glycosidic bond angle was increasd to a value of 120°, which lies in the range observed in the solid state (see Table I). This increase does not modify the calculated molecular energy for the conformation of crystalline sucrose but allows greater flexibility when conformational analysis is carried out with rigid residues.[43] The same procedure provided a starting model for 2-deoxysucrose after the O-2g hydroxyl group was replaced by a hydrogen atom. Both pyranosyl rings retained unaltered $^4C_1$ shapes, and the fructofuranoysl rings took forms close to $^4T_3$.

After the starting geometry was developed with MMP2(85), the program PFOS (Potential Function for Oligosaccharide Structures)[44,45] was used to systematically calculate the intramolecular energy at 5 degree increments of Φ and Ψ. The sugar residues remained rigid, and the energy is the sum of terms from van der Waals[46] interactions, torsional rotations, and exo anomeric effects.[47] A function for interresidue hydrogen bonds,[48] based on oxygen–oxygen distances, is optional. Individual energy maps, with and without hydrogen bonding, were prepared for both sucrose and its deoxy analogue, by using combinations of primary alcohol group orientations that occur in the crystal structure literature. For ωg and ωf, the observed orientations are GT and GG, while for χf, they are TG and GG. The individual maps are identified by their primary alcohol orientations in the order of O-6g, O-6f, and O-1f; i.e., their names are GG–GG–GG, GG–GT–GG, GT–GG–GG, GT–GT–GG, GG–GG–TG, GG–GT–TG, GT–GG–TG, and GT–GT–TG. Thus, a total of 16 maps were calculated for each disaccharide.

Table III. Observed NOEs Values for Sucrose and 2-Deoxysucrose in Aqueous Solution

saturated proton	intraresidue NOE (%)		interresidue NOE (%)	
		Sucrose		
H-1g	H-2g	(18.0)	H-1f	(7.0)
			H-4f	(0.7)
H-2g	H-1g	(12.2)		
	H-4g	(6.5)		
H-3g	H-4g	(2.5)		
H-4g	H-2g	(14.4)		
	H-3g	(4.3)		
	H-6g + H6f	(2.4)		
H-1f	H-3f	(7.0)	H-1g	(9.5)
H-3f	H1-f	(3.0)		
	H-5f	(6.0)		
H-4f	H-6g + H6f	(4.5)	H-1g	(1.5)
		2-Deoxysucrose		
H-1g	H-2ga	(5.0)	H-1f	(5.0)
	H-2ge	(2.5)	H-4f	(2.2)
H-2ga	H-1g	(10.5)		
	H-2ge	(22.0)		
	H-4g	(11.0)		
H-2ge	H-1g	(5.5)		
	H-2ga	(27.0)		
	H-3g	(15.0)		
H-3g	H-2ge	(4.0)		
	H-4g	(4.5)		
H-4g	H-2ga	(3.5)		
	H-3g	(4.5)		
H-1f	H-3f	(7.0)	H-1g	(6.5)
H-3f	H-1f	(2.0)		
	H-5f	(6.5)		
H-4f	H-5f	(4.5)	H-1g	(1.5)
	H-6g + H6f	(3.5)		

Results and Discussion

NMR Data. Both ^1H and ^{13}C chemical shifts for sucrose have been previously assigned,[10,12] and the ^1H chemical shifts for 2-deoxysucrose were obtained from the COSY spectrum. These ^1H chemical shifts, the ^1H T_1s and the $^3J_{H-H}$ of sucrose which are similar to literature values, and the $^3J_{H-H}$ of 2-deoxysucrose are collected in Table II. Correlation times of 1.2×10^{-10} and 1×10^{-10} s were obtained for sucrose and 2-deoxysucrose, respectively (for the tubes used in the NOE studies), from the average ^{13}C T_1 value of the methine carbons and a proton–carbon distance, r_{C-H}, of 0.11 nm by using the equation

$$\frac{1}{T_1} = \left(\frac{\mu_0}{2\pi}\right) \frac{\hbar^2 \gamma_C^2 \gamma_H^2}{10 r_{C-H}^6} \left(\frac{\tau_c}{1 + (\omega_H - \omega_0)^2 \tau_c^2} + \frac{3\tau_c}{1 + \omega_c^2 \tau_c^2} + \frac{6\tau_c}{1 + (\omega_H + \omega_c)^2 \tau_c^2} \right)$$

where $\hbar$ is Planck's constant divided by 2π, and γ_C and γ_H are the carbon and proton gyromagnetic ratios.

Conformation of The Glucopyranosyl Ring. Both coupling constants and NOE can give indication about ring conformation. For the glucose ring, theoretical $^3J_{H-H}$ values calculated from Altona's empirical equation[49] for a classical $^4C_1$ ring form are reported in Table II. The comparison with the observed values shows maximum deviations of 0.3 and 0.5 Hz for sucrose and 2-deoxysucrose, respectively. $^3J_{C\cdot3g-H\cdot1g}$ and $^3J_{C\cdot5g-H\cdot1g}$ values of 6.0 and 7.1 Hz were obtained from selective heteronuclear 2D-J NMR. These coupling constants indicate torsion angles of about 180°, compatible with the $^4C_1$ form. The intraresidue NOE values

(42) Allinger, N. L. *J. Am. Chem. Soc.* **1977**, *99*, 8127–8134.
(43) Brant, D. A.; Christ, M. D.; In *Computer Modeling of Carbohydrate Molecules*; French A. D., Brady, J. W., Eds.; ACS Symposium Series; American Chemical Society: Washington, DC, 1990; pp 42–68.
(44) Perez, S. D.Sc. Thesis, Grenoble, France, 1978.
(45) Tvaroska, I.; Perez, S. *Carbohydr. Res.* **1986**, *149*, 389–410.
(46) Scott, R. A.; Scheraga, H. A. *J. Chem. Phys.* **1966**, *44*, 3054–3069.
(47) Tvaroska, I. *Carbohydr. Res.* **1984**, *125*, 155–160.
(48) Perez, S.; Vergelati, C. *Polymer Bull.* **1987**, *17*, 141–148.
(49) Altona, C.; Haasnoot, C. A. G.; *Org. Magn. Reson.* **1980**, *13*, 417–429.

measured for the glucosyl moieties, Table III, agree well with expected values for the $^4C_1$ chair conformation[50] although some of the observed values were unacceptably small due to the lack of selectivity of the saturating field (i.e., NOE value for H-4g upon irradiation of H-2g). A weaker irradiating field improved these values somewhat (values in Table III).

Conformation of the Fructofuranosyl Ring. Previous NMR work on sucrose[9,12] indicated that the fructosyl residue is flexible in solution, especially at C-3 and C-4. This agrees with a recent molecular mechanics[51] study that showed that the overall minimum and the ^2E, $^2T_3$, E_3, $^4T_3$, ^4E, and $^4T_5$ conformations were bound by the 2 kcal/mol contour, within which facile pseudorotation is likely. That prediction was supported by the observation that the fructofuranosyl moiety in most crystal structures fell in that range.

Our observed values for $^3J_{H\text{-}3f\text{-}H\text{-}4f}$ and $^3J_{H\text{-}4f\text{-}H\text{-}5f}$ of 8.8 and 8.3 Hz can be correlated respectively with torsion angles of approximately 170° and −160°, by using equations established by the method proposed by Hasnoot et al.[52] (see bottom of Table II). These angles correspond to a shape between $^4T_3$ and ^4E. In Table II, the calculated coupling constants for sucrose and deoxysucrose are based on the starting structures optimized with MMP2(85). The 1-Hz discrepancy is not particularly significant, since the H-3f–H-4f coupling constant changes rapidly with small angular changes in this region. The very small coupling constant measured for $^3J_{C\text{-}5f\text{-}H\text{-}3f}$ can correspond to a torsion angle near 180°, also compatible with an average conformation between $^4T_3$ and ^4E.

Interresidue Conformation. When irradiating H-1g, two interresidue NOEs, H-1g/H-1f and H-1g/H-4f, are observed. With the exception of the latter interresidue effect and the NOE measure for H-1g upon saturating H-1f (9.5% instead of 6.5%), the values reported in Table III are similar to the partial NOE data reported earlier[12] for sucrose. The phase-sensitive NOESY spectrum of sucrose acquired with a mixing time τ_m of 1.25 s, Figure 2, contains all the crosspeaks corresponding to the NOE effects measured in the 1D spectrum. In order to visualize the weak H-1g/H-4f crosspeak, the sums of the corresponding slices in both ω_1 (insert) and ω_2 (below) have been amplified and integrated. Although the H-1g/H-1f and H-1g/H-4f crosspeaks could be detected for short mixing times ($\tau_m > 0.1$ s), low sensitivity precluded quantitative measurements of the initial NOE buildup rate. In the case of H-2g and H-4g, the two interresidue NOEs observed in the present work have been reported by Sanders and Hunter[53] for sucrose octaacetate. The value of $^3J_{C\text{-}2f\text{-}H\text{-}1g}$ measured for sucrose, 4.2 Hz, is similar to the one reported by Mulloy et al.,[10] 3.8 Hz, and differs from the value, 5.3 Hz, predicted for the crystal structure by these authors with use of a Karplus-type relationship. Again, as NMR parameters reflect virtual conformations, this suggests that aqueous sucrose is not adequately described by the crystal conformation.

Molecular Modeling. Of the primary alcohol group orientations, only the positions of O-1f have much effect on the potential energy surfaces. The maps for GT–GT–GG are shown in Figure 3a,b, and the maps for GT–GT–TG are in Figure 3c,d. In Figure 3c,d, the zones of potential hydrogen bonds are indicated, and the location of each low-energy minimum (S1–S5) is shown in Figure 3c. The main effect of the O-1f position is on the S3 minimum. On the GT–GT–TG maps, the S3 minimum is isolated from the other four minima, and the energy is higher than on the corresponding GT–GT–GG maps.

Maps computed with and without the hydrogen-bonding potential have the same number and locations of minima. Therefore, it appears that intraresidue hydrogen bonding plays at most a minor role in determining the conformation of isolated sucrose molecules. This minor role might include deepening of the S3, S4, and S5 wells, while the depths of the S1 and S2 wells are unaffected. The crystallographically observed O-1f–O-2g bond appears on the edge of the S2 zone and extends this zone somewhat compared to the map made without hydrogen bonds. This bond can occur only when O-1f has a TG orientation. Hydrogen bonds involving O-6g or O-6f are not indicated on the energy maps or the molecular drawings.

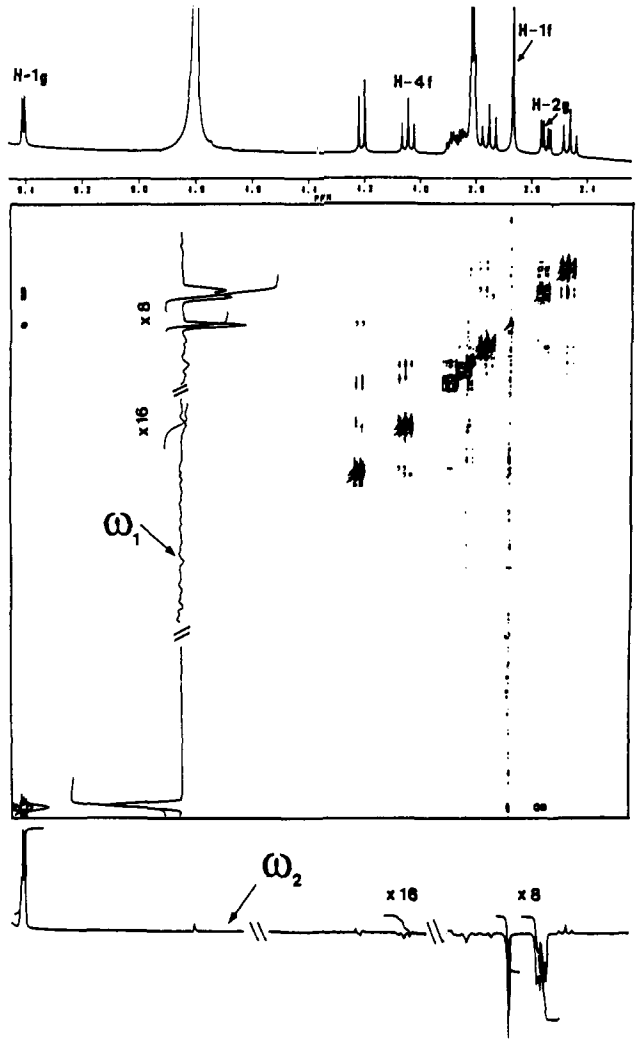

Figure 2. Unsymmetrized, phase-sensitive 400-MHz ^1H NOESY spectrum of 0.06 M sucrose in D_2O (δ_{DOH} = 4.8 ppm). On the corresponding 1D spectrum (above) H-1g, H-4f, H-1f, and H-2g are labeled. Summed ω_1 (insert) and ω_2 (below) subspectra with H-1g on the diagonal are also given.

Figure 4 displays the analogous energy maps and structural drawings for 2-deoxysucrose. The main difference between Figures 4a and 3a is the appearance of a new, low-energy region labeled D6 that can occur when O-1f has a GG position. The drawing labeled D6GG shows that this conformer exists owing to the replacement of the hydroxyl group at C-2g by a less bulky hydrogen atom, allowing closer approach of the two residues. Even less influence from interresidue hydrogen bonding is observed for 2-deoxysucrose. Only D3 and D4 can form hydrogen bonds (again, hydrogen bonds involving O-6g and O-6f are not considered).

Combination of NMR and Modeling Results. The observed interresidue NOE values and $^3J_{C\text{-}H}$ are compared in Table IV with values computed from the low-energy conformers of sucrose having O-1f in GG and TG positions. Table IV also includes some interesting intraresidue NOEs. The range (0.1–26%) for the NOE calculated for H-4f when H-1g is saturated shows how sensitive NOEs can be to the glycosidic linkage conformation. In contrast, the intraresidue H-2g NOE is almost constant.

Of the individual low-energy forms, S3 GG provides calculated NOEs that agree best with the observed values in Table IV, but

(50) Dais, P.; Perlin, A. S. *Adv. Carbohydr. Chem. Biochem.* **1987**, *45*, 125–168.
(51) French, A. D.; Tran, V. *Biopolymers* **1990**, *29*, 1599–1611.
(52) Haasnoot, C. A. G.; De Leeuw, F. A. A. M.; Altona, C. *Tetrahedron* **1980**, *36*, 2783–2792.
(53) Sanders, J. K. M.; Hunter, B. K. In *Modern NMR Spectroscopy. A Guide for Chemists*; Oxford Press University: 1987; pp 282–297.

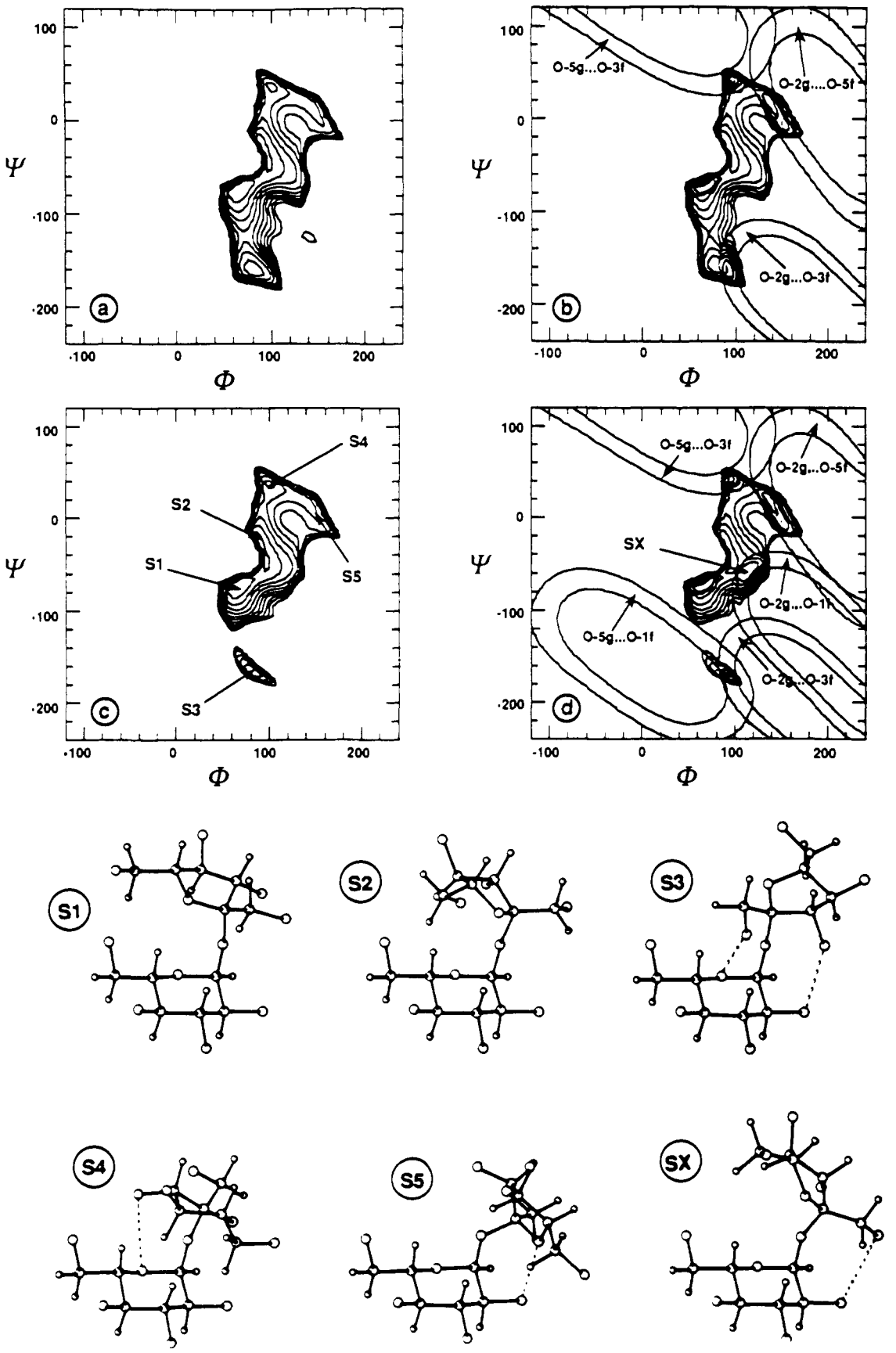

Figure 3. Isoenergy maps of the sucrose molecule as a function of the Φ and Ψ torsion angles. The hydroxymethyl groups were fixed in the orientations GT–GT–GG (referring to ωg–ωf–χf) in panels a and b and GT–GT–TG in panels c and d. Energies in panels b and d include hydrogen bond contributions. In all cases, isoenergy contours are drawn at increments of 1 kcal/mol with respect to the absolute minimum. The drawings of the five low-energy conformers (S1–S5) referred to Φ and Ψ values labeled on map 4c. The crystal structure conformation (SX) also is labeled on map 3d.

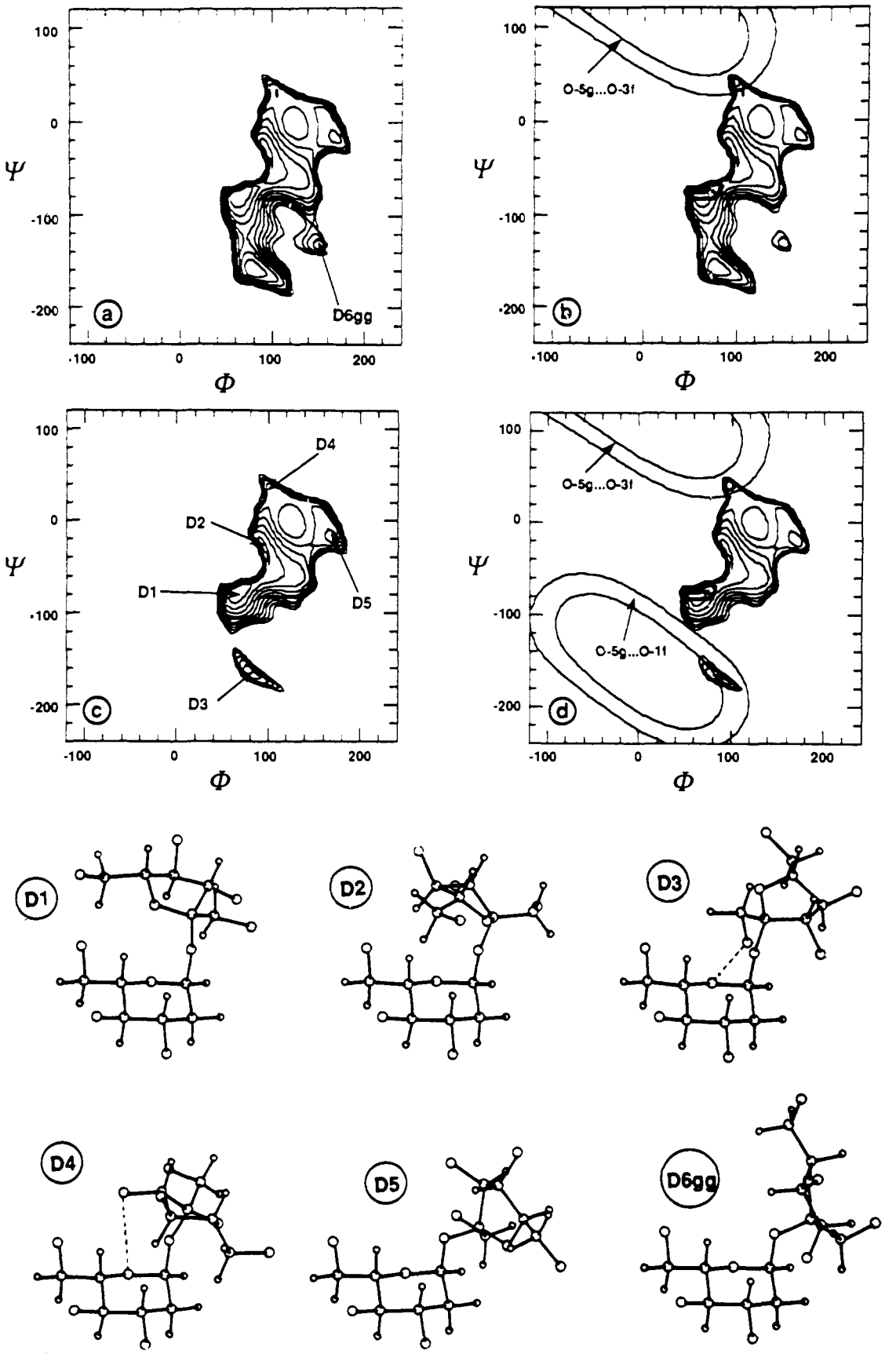

Figure 4. Isoenergy maps of the 2-deoxysucrose molecule as a function of the Φ and Ψ torsion angles. The different panels have the same legends as in Figure 4. The drawings of the five low-energy conformers corresponding to a TG orientation of χf (D1–D5) referred to Φ and Ψ values labeled on map 4c; the conformer S6, with a GG orientation of χf, is labeled in Figure 4a.

the 2.6% difference for the H-1f*–H-1g NOEs is not satisfactory. Figure 5 depicts the conformational zones wherein the values of two observed interresidue NOE would agree with the observed values, superimposed on the maps of conformational energy for the GG and TG positions of O-1f. The failure of these zones to intersect shows that there is no Φ,Ψ combination that can si-

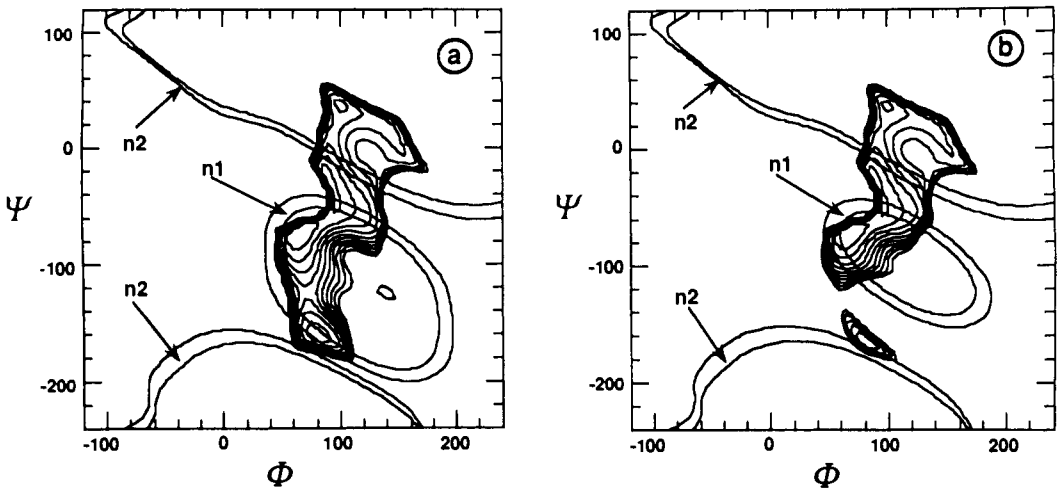

Figure 5. NOE contour surfaces superimposed on isoenergy maps of the sucrose molecule. The hydroxymethyl groups are in the orientation GT–GT–GG (referring to ωg–ωf–χf) and GT–GT–TG in panels a and b, respectively. The isoenergy contours are drawn as in Figure 3. Two NOE contour surfaces are displayed. They are limited by two iso-NOE contours corresponding to the observed value ±20%. The NOE effect observed for H-1f upon saturation of H-1g (0.07) is n1, and n2 is the NOE effect observed on H-1g upon saturation of H-4f (0.015).

Table IV. NOE Values (%) and $J_{H\text{-}1g\text{-}C\text{-}2f}$ Coupling Constant (Hz) Calculated for Some Low-Energy Minima of the Sucrose Molecule and for Average Over All the Potential Energy Surfaces[a]

		S1		S2		S3		S4		S5		AM	AMH	exptl
χ^f		GG	TG	GG	TG	GG	TG	GG	TG	GG	TG			
Φ		65	70	90	90	80	80	100	100	150	150			
Ψ		−75	−70	−25	−25	−160	−165	40	40	5	5			
							NOE Values							
(s)[b]	(d)[c]													
H-1g	H-1f	12.2	10.6	2.4	2.2	6.9	0.7	0.2	0.2	0.3	0.2	7.0	7.0	7.0
	H-4f	0.2	0.1	0.3	0.3	0.8	1.0	26.2	26.1	15.7	15.7	1.1	1.1	0.7
	H-2g	18.9	19.0	19.0	19.1	18.9	19.2	18.1	18.1	18.3	18.3	19.1	19.1	18.0
H-1f	H-1g	15.3	15.1	5.8	5.3	12.1	2.1	0.2	0.2	0.3	0.2	11.3	11.3	9.5
	H-3f	5.9	10.2	5.9	10.2	5.3	9.8	5.8	10.1	5.9	10.3	8.6	8.6	7.0
H-4f	H-1g	0.1	0.1	0.5	0.5	0.4	1.0	17.9	17.9	9.2	9.3	0.8	0.8	1.5
							Coupling Constants							
$J_{H\text{-}1g\text{-}C\text{-}2f}$		2.3	2.7	4.5	4.5	3.7	3.7	5.1	5.1	4.0	4.0	3.5	4.1	4.2

[a] AM and AMH, averaging over all maps without and with the contribution of hydrogen bonds, respectively; exptl, experimental values. [b] (s) saturated proton. [c] (d) detected proton.

Table V. Values (%) Calculated for Some Low-Energy Minima of the 2-Deoxysucrose Molecule and for Averaging for All the Potential Energy Surfaces[a]

		D1		D2		D3		D4		D5		D6	AM	AMH	exptl
χ^f		GG	TG	GG	TG	GG	TG	GG	TG	GG	TG	GG			
Φ		65	65	90	90	80	80	105	100	170	170	155			
Ψ		−80	−80	−20	−20	−160	−165	30	40	−20	−20	−135			
								NOE Values							
(s)[b]	(d)[c]														
H-1g	H-1f	13.3	9.8	1.8	1.7	7.3	0.7	0.2	0.1	0.1	0.0	17.5	6.7	6.7	5.0
	H-4f	0.2	0.2	0.4	0.4	0.9	1.2	21.6	29.4	8.2	6.2	0.2	1.3	1.3	2.2
	H-2ge	2.7	2.7	2.7	2.7	2.7	2.7	2.7	2.7	2.2	2.0	1.4	2.4	2.4	2.5
	H-2ga	4.4	4.4	4.4	4.4	4.4	4.4	4.3	4.2	4.5	4.6	4.6	4.5	4.5	5.0
H-1f	H-1g	13.9	12.6	3.2	2.9	10.3	1.5	0.1	0.1	0.1	0.1	15.3	8.9	8.9	6.5
	H-3f	5.6	10.5	5.7	10.5	5.2	10.2	5.6	10.4	5.7	10.5	5.0	8.7	8.7	7.0
H-4f	H-1g	0.1	0.1	0.5	0.5	0.4	0.8	9.5	16.5	4.0	3.2	0.1	0.7	0.7	1.5
	H-5f	3.5	3.6	3.6	3.6	3.7	3.7	3.3	3.2	3.5	3.5	3.7	3.3	3.3	4.5

[a] AM and AMH, averaging over all maps without and with the contribution of hydrogen bonds, respectively; exptl, experimental values. [b] (s) as in Table IV. [c] (d) as in Table IV.

multaneously generate both enhancements.

Therefore, some sort of conformational averaging over the five low-energy conformers is required to explain the NMR results. A simple averaging of the values for the five conformers does not suffice, and complete integration over all the maps, described in the methods section, was then employed. Those averages are given in Table IV under the headings AM and AMH, based on the maps without and with hydrogen bonding, respectively. The NOEs were not affected by the presence or absence of hydrogen bonding in the maps used for averaging, but the coupling constants fit the experiment better when hydrogen bonding was included. Overall, the AMH values correspond reasonably well with the experimental results.

The NOE value observed for H-3f upon irradiation of H-1f is influenced by variations in the O-1f hydroxymethyl group orientation but not by variations in the conformation at the glycosidic

linkage (Table IV). This NOE effect has values of 6% for the GG position and 10% for the TG position, so both positions must be considered to explain the observed value of 7%. The GT position of O-1f gives values above 11%, justifying its omission from the above analyses.

Table V reports values analogous to those in Table IV for 2-deoxysucrose. Again, there is no satisfactory fit between the values calculated for any single conformer and the experimental results. The bases for this conclusion are the variations in NOEs for H-1f and H-4f that are observed when H-1g is saturated and the variation in the NOE for H-1g when H-1f is saturated. The averaged predicted values, invariant with the presence or absence of hydrogen bonding, again provide a better agreement with the experimental results.

Hydrogen Bonding. The potential energy surfaces and the NMR data for sucrose are strikingly similar to the surfaces and data of the 2-deoxy analogue. Thus, the crystallographically observed O-1f–O-2g hydrogen bond must not significantly influence the solution conformation of sucrose. Exchange of hydrogen-bonding partners between the neighboring intramolecular hydroxyl groups and solvent water is probably a factor, but sucrose also has an unusual relationship between the energetically accessible conformations of the glycosidic linkage and conformations that allow interresidue hydrogen bonds. The disaccharides maltose and cellobiose have large intersections of energetically accessible areas that can be further stabilized by hydrogen bonds, where Figures 3b,d and 4b,d show that only minor portions of the allowed domains for sucrose are compatible with hydrogen bonding.

Figure 3d also demonstrates that, in regard to the hydrogen bonding proposed for DMSO solutions,[6] with O-2g bonding to either O-1f or O-3f, these two bonds cannot occur with the same conformation of the glycosidic linkage.

Comparison with Relaxed Residue Mapping. Recently, "relaxed residue" conformational analyses of disaccharides[23,24,55-57] have been reported. In relaxed maps, the individual atomic positions are allowed to adjust at each increment of the glycosidic linkage torsion angles, thereby relieving any artificial contribution to the calculated energy that results from residue rigidity. The relaxed map of sucrose[23,24] is consistent with our rigid maps in terms of overall shape and location of the minima but is better for understanding the pathways of conformational interchange among the minima. These intuitively superior, relaxed energy maps have been criticized[43] for depicting regions of low energy that are too extensive, compared to experimental values in aqueous solution. In studies such as the present one, where solvent is not explicitly considered, it may be that rigid residue analysis provides a more realistic result.

Conclusions

In regards to the NMR data of sucrose, the major difference between the present study and previous one[12] is the observation of a small interresidue NOE. This dipolar interaction, which was observed for a wide range of mixing times, is not compatible with the conformation observed in crystalline sucrose. While the crystalline form has been considered to be the sole conformation in aqueous solution,[8,9,12] our studies show that weighted average NOE and coupling constants, computed over all energy maps, provide better agreement with experiment.

The influence of hydrogen bonds on the solution behavior of sucrose requires special attention because of its presumed importance as well as the controversial interpretation of the results stemming from different techniques. Because conformational maps varied little regardless of whether hydrogen-bonding potentials were included, we conclude that hydrogen bonding is not important in determining conformations of sucrose in aqueous solution. This was supported by the strong similarity of the conformational maps for sucrose with those of the deoxy analogue which is unable to form the crystallographically observed hydrogen bond. The NOE and coupling constant data observed for the two molecules are also similar, further refuting the importance of hydrogen bonding in aqueous solution.

Acknowledgment. The authors are much endebted to Prof. J. Carver and Tom Lew (University of Toronto) for access to the computer programs for the calculation of the NOE values and graphic representation of the energy maps. Appreciation is extended to Dr. A. D. French (USDA, New Orleans) for his careful reading of the manuscript. Financial support from the Pierre et Marie Curie University, the CNRS (UA 1110), and the INRA is acknowledged. One of us (N.R.) acknowledges the support from French Ministry of Research and Technology.

Registry No. Sucrose, 57-50-1; 2-deoxysucrose, 6852-68-2.

(54) Pangborn, W.; Langs, D.; Perez, S. *Int. J. Biol. Macromol.* **1985**, *7*, 363–369.
(55) Tran, V.; Buleon, A.; Imberty, A.; Perez, S. *Biopolymers* **1989**, *28*, 679–690.
(56) French, A. D. *Carbohydr. Res.* **1989**, *188*, 206–211.
(57) Imberty, A.; Tran, V.; Perez, S. *J. Comput. Chem.* **1989**, *11*, 205–216.